

Assessing the bond strength of expansive agent-enhanced repair mortars for ageing concrete structures

Lina Ammar, Kinda Hannawi, Aveline Darquennes*

Univ Rennes, INSA Rennes, LGCGM (Laboratoire de Génie Civil et Génie Mécanique) – France

Abstract. As reinforced concrete structures age, they increasingly require extensive maintenance and repair. Due to their limited lifespan, repair materials are often susceptible to early cracking, resulting from environmental influences, deformation, and physical-chemical incompatibilities between the repair material and the substrate. In line with sustainable development goals, minimising costly maintenance and repairs is essential. Self-healing mortar presents a promising solution to extend the durability of repaired structures and reduce long-term maintenance needs. The primary objective of this research is to evaluate the self-healing capacity of a cementitious material containing magnesium oxide and calcium sulfo-aluminate-based expansive agents, as well as to assess its mechanical performance under repair conditions. Healing kinetics are monitored through water permeability tests on cylindrical specimens precracked at 28 days. To validate the suitability of the studied mortars for repair applications, their bond strength is measured using pull-off tests under various concrete substrate conditions, including different roughness and saturation levels. Experimental results indicate that incorporating an expansive agent enhances the autonomous healing potential of mortars, with mortars containing calcium sulfo-aluminate-based expansive agents demonstrating superior bond strength and a better healing capacity.

1 Introduction

Many risks affecting civil engineering structures are typically managed by engineers using design and construction standards that generally ensure sufficient safety. However, unforeseen risks can arise due to environmental, mechanical, and other conditions [1,2]. Cement-based materials experience volumetric changes due to chemical, thermal, microstructural evolution, and interactions with their environment when in contact with water. When they are restrained, these deformations can lead to cracking in concrete structures [3], altering local transfer parameters and allowing water and aggressive agents to penetrate more easily, damaging the cement matrix and affecting the structure's durability. This can result in high repair costs and socio-economic and environmental impacts. Therefore, there is a need for more environmentally friendly and durable repair solutions.

In civil engineering, certain solutions can reduce crack formation in structures. One approach that has gained attention is the use of self-healing materials [4,5]. Self-healing is defined as a material's ability to repair its own cracks over time. Two main self-healing mechanisms are autogenous healing, which occurs through the hydration of anhydrous grains or carbonation of hydration products, and autonomous healing, which involves adding specific materials like expansive agents to enhance the self-healing capacity of cracks. Expansive agents (EAs) are commonly used in concrete and mortar mixtures to reduce shrinkage and have recently been explored for their self-healing properties due to their ability to form expansive

hydration products. Formulations with EAs, such as magnesium oxide (MgO) or calcium sulfo-aluminate (CSA), have shown self-healing properties in some studies [4, 6-9]. However, most of these studies have focused on the self-healing process of pre-cracked samples at an early age (e.g., 1 day) with initial crack openings of less than 170 μm [6-9]. It is important to note that self-healing at an early age can be enhanced even without EAs due to the presence of more unhydrated particles in the crack [5]. Additionally, the healing capacities demonstrated in these studies are limited to autogenous healing, with no verification of autonomous healing.

The primary objectives of this study are to design repair mortar mixtures containing expansive agents (EAs) and propose an experimental campaign to achieve our research goals. We aim to evaluate the impact of EAs on the compressive strength of cement-based mortar mixtures to ensure compliance with repair standards such as EN 1504-3 [10]. Additionally, we will investigate some delayed deformations, a key material parameter influencing the cracking sensitivity of repair mortars and giving us information on the autonomous healing capacity.

Furthermore, the study will assess the self-healing process and kinetics of cracked specimens for the proposed mortar mixtures, determining the limits of autonomous healing. Specifically, we will focus on using MgO and CSA to evaluate their autogenous and autonomous healing capabilities beyond 28 days on crack width ranges varying from 50 to 400 μm . Lastly, we will examine the interactions between the repair mortar and a sound concrete matrix through bond

strength tests. A parametric study will be conducted to consider the effects of surface preparation, including water content and roughness, on bond strength. By addressing these objectives, the study aims to develop effective and durable repair mortars that meet industry standards and exhibit enhanced self-healing capabilities.

2 Materials

Two types of repair mortars with expansive agents (EAs) were selected for this study: one based on magnesium oxide (MgO) and the other on calcium sulfo-aluminate (CSA). Each expansive agent constitutes 5 % of the cement weight. These mortars are named as MG5 and CSA5, respectively. The mixture proportions are detailed in Table 1. The water-to-binder and sand-to-binder ratios are kept constant at 0.45 and 2, respectively.

All mortar mixtures exhibit sufficient fluidity for future repair applications. To achieve this, the superplasticiser Sika ViscoFlow-800 Power is used, with its content specified in Table 1 for each mixture (by binder weight). For the specimens used to monitor the healing process, steel fibres (50 kg/m³) are added to better control the initial crack width. These fibres have a length of 25 mm and a diameter of 0.2 mm.

Table 1. Compositions of the repair mortars and support concrete (kg/m³).

	MG5	CSA5	CS
CEM I 52.5 N	619	616	395
EA	33	32	-
Sand, 0/4 mm	1299	1299	761
Aggregates, 4/8 mm	-	-	1037
Water	292	292	178
Superplasticiser (%)	0.3	0.3	-

The Concrete Support (named CS - Table 1) for bond strength tests is formulated using CEM I 52.5 N cement, and its composition, optimised with the Dreux-Gorisse method, is of type MC45 according to [10]. This means the mixture must have a cement content between 395 kg/m³ and 410 kg/m³ and a water-to-cement ratio of 0.45. This concrete also respects the exposure classes XS3 (chloride-induced corrosion of reinforcement from seawater) and XC4 (carbonation-induced corrosion) as defined in the EN 206 standard [11].

3 Experimental methods

3.1 Mechanical performance

To understand the impact of EAs on mortar behaviour and to further explain the self-healing results, the mortar's deformation was monitored. Measurements were conducted on prismatic specimens (4 × 4 × 16 cm³) stored under two curing conditions at 20 ± 1 °C (3 specimens per curing condition) during 100 days:

- Autogenous curing: Specimens were sealed with a double layer of aluminium foil to prevent moisture loss.
- High relative humidity curing: Specimens were stored at 95 ± 5 % R.H. for 28 days, followed by water curing (WC). This curing condition was chosen to reproduce the conditions used for self-healing evaluation, allowing the results to be used to explain the self-healing outcomes.

Deformations were monitored from 1 day onward using a retractometer with a precision of 1 µm. The interactions between the specimens and their environment were tracked by measuring mass variations.

The compressive strength was measured on three specimens at 28 days, in accordance with the European standard EN 196-1 [12]. Prior to testing, the specimens were stored in a humid chamber at 95 ± 5 % Relative Humidity (R.H.) and 20 ± 1 °C.

3.2 Self-healing evaluation

To evaluate the self-healing capacity of the mixtures, Water Permeability (WP) tests were conducted to achieve a 3D monitoring of crack healing. For each composition, two cylindrical specimens with a diameter (Φ) equal to 11 cm and a height (h) of 20 cm were prepared. After demoulding, the specimens were stored in a humid chamber (R.H. = 95 ± 5 %, 20 ± 1 °C) until they reached the cracking age of 28 days. Three days before the test (at 25 days), each cylindrical specimen was cut into three disks (h = 5 cm). At 28 days, all disks were pre-cracked using a splitting test to achieve a crack width of 0.2 ± 0.05 mm. During the splitting test, the crack opening was visually controlled thanks to a specific ruler (Figure 1a).

Subsequently, the PVC tubes were filled with water. To monitor the water flow through the crack, the specimens were placed on a support above a balance (Figure 1b). The quantity of water that flowed through the specimen was measured after 5, 10, 15, 20, 25, and 30 minutes to quantify the water flow rate (l/m) across three disks per composition. The water permeability test was conducted immediately after cracking (0D), and then after 7 days (7D), 25 days (25D), and 112 days (112D) of curing.



Fig. 1. Crack width controlled with a ruler during the splitting test (a), Water Permeability test (b).

After the WP test, all disks were stored vertically in a container filled with water (one container per mixture). From each curing condition, a Self-Healing Rate ($SHR(t)$) was calculated according to Equation (1):

$$SHR(t) = \frac{WF(0D) - WF(t)}{WF(0D)} \times 100 \quad (1)$$

Where: $SHR(t)$ is the Self-Healing Rate at time t (%), $WF(0D)$ is the initial water flow just after the cracking at the time named '0D' (l/min); and $WF(t)$ is the water flow after a healing period t (l/min).

3.3 Bond strength measurement

Bond strength measurement through direct tensile testing is conducted using the pull-off test method (Figure 2). This test is recommended by the standard for repair products [10] and is performed according to the procedure described in the NF EN 1542 standard [13]. The test method involves drilling a core through the repair layer and the interface into the substrate, bonding a cylindrical steel transfer plate to the top of the core with a suitable adhesive (epoxy glue), and then pulling on the plate until the core is detached. During the test, the loading rate was maintained continuously and steadily at 0.05 ± 0.01 MPa/s until failure occurred. When the failure occurs in the interface zone between the repair layer and the substrate, the bond strength (f_{bd}) is calculated with Equation (2).



Fig. 2. Measurement of bond strength by the pull-off test method.

$$f_{bd}(MPa) = \frac{4 \cdot F_{max}}{\pi \cdot D} \quad (2)$$

Where: F_{max} is the failure load (N), and D is the specimen mean diameter (mm).

To conduct bond strength tests, concrete prisms measuring $30 \text{ cm} \times 25 \text{ cm} \times 7.5 \text{ cm}$ were used as the concrete support (CS). The influence of the roughness and water content of the upper surface ($30 \text{ cm} \times 25 \text{ cm}$) of these specimens on the interface between the repair mortar and the support concrete was studied. Roughness was achieved through mechanical treatment by grinding (GS) or chemical treatment with a setting retarder sprayed on the surface (DS) of freshly poured concrete (Figure 3). After obtaining the desired roughness, the surface was cleaned to remove loose particles (debris, dirt, grease, or other surface contaminants) that could affect the bond between the concrete and mortar. The surfaces were brushed and then blown with compressed

air. The methods for characterising the roughness of the concrete support are described in the next paragraph.

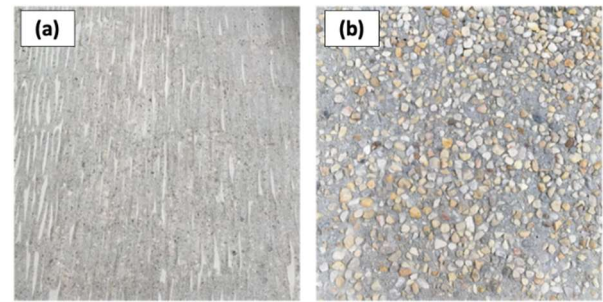


Fig. 3. Roughness of the support concrete: ground surface (GS) (a) and surface after chemical treatment (DS) (b).

Once matured, the concrete specimens were placed in a climate-controlled chamber at 75 % and 85 % R.H. until the samples reached complete stabilisation. Subsequently, the repair mortars were cast in a 2.5 cm layer onto the treated and cleaned surface of the support concrete. The assembly was then cured at 20 °C and 95 % R.H. for 50 days before conducting the direct tensile bond strength test.

3.4 Roughness Measurement

One of the most commonly used methods for characterising surface roughness is the sand patch test, as described in the NF EN 13036-1 standard [12]. This method measures the average peak height, known as the Mean Profile Depth (MPD), of a horizontal surface. To perform the test, a determined volume of standardised sand ($V = 25 \text{ ml}$) is uniformly spread over the surface. As the sand is spread, it fills the "valleys" of the texture, forming a circular patch known as a "sand patch". The diameter of the circular area covered by the sand is measured at a minimum of four equidistant points around the circumference. From the average diameter D , the mean texture depth can be calculated using Equation (3).

$$MPD = \frac{4 \cdot V}{\pi \cdot D^2} \quad (3)$$

The advantage of this method is that it is quick, cost-effective, and straightforward to execute. To obtain representative results, a set of five measurements is taken on three different plates ($50 \text{ cm} \times 50 \text{ cm} \times 5 \text{ cm}$) for each type of roughness.

To better understand the geometry of roughness, observations were conducted using a 3D optical microscope to determine the profile for each type of roughness tested. The following roughness parameters were determined based on the articulated comb method proposed by [15]: the wavelength (λ), which is the average distance between two irregularities, and the double average amplitude ($2a$), which is the average height between successive peaks and valleys over the considered length.

3.5 Microstructure characterisation

To understand the results at the macroscale, the hydration products were characterised using several

techniques: thermogravimetric analysis (TGA) performed on specimens aged from 3 to 90 days, and X-ray diffraction (XRD) analysis conducted on 28 day old paste specimens. The specimens were stored at $95 \pm 5\%$ R.H. and $20 \pm 1\text{ }^\circ\text{C}$ for the first 28 days and then cured in water beyond 28 days.

Additionally, the self-healing products formed within the cracks were identified using Scanning Electron Microscopy (SEM) analysis. After one year, the disks were cut into 2×2 cm cubes around the crack.

4 Results and Discussion

4.1 Mechanical Performances

All mixtures meet the requirements of the European standard EN 1504-3 [10], as shown in Table 2. The standard classifies mortars into non-structural (R1 and R2) and structural (R3 and R4) categories. All the mortars studied in this chapter are classified as R4, with a compressive strength of ≥ 45 MPa. The addition of MgO and CSA slightly reduces the compressive strength compared to a reference mortar without expansive agents (69.9 ± 2.9 MPa at 28 days) [16]. This reduction is partly attributed to the lower cement content, due to its partial replacement by expansive agents, as well as to the nature of the hydration products formed by the expansive agents.

Table 2. Compressive strength at 28 days.

	MG5	CSA5
$f_{c,28d}$ (MPa)	63.4 ± 1.0	68.2 ± 2.0

The results of autogenous deformation are presented in Figure 4. The mass variation of all specimens is less than 0.02 %, confirming the autogenous conditions of the specimens. The addition of 5 % EAs reduces autogenous shrinkage. Specifically, the shrinkage values at 7 days are $-72\text{ }\mu\text{m/m}$ for MG5 and $-165\text{ }\mu\text{m/m}$ for CSA5. In comparison, the reference mortar without expansive agents exhibits a shrinkage of $-324\text{ }\mu\text{m/m}$ at the same age [16]. However, CSA5 shrinks faster than MG5.

The rapid hydration of CSA produces ettringite at an early age, as shown by the XRD results [16], initially reducing the autogenous shrinkage of CSA5. Conversely, the slower hydration of MgO [16] continues to form brucite over the long term, which accelerates the reduction of autogenous shrinkage. Consequently, MG5 exhibits a relatively constant autogenous shrinkage beyond 20 days, stabilising at around $-105\text{ }\mu\text{m/m}$. In contrast, CSA5 continues to shrink until 28 days, reaching $-300\text{ }\mu\text{m/m}$, and then remains relatively constant at around $-315\text{ }\mu\text{m/m}$ beyond 28 days. By comparison, the autogenous shrinkage of the reference mortar without expansive agents stabilises at approximately $-450\text{ }\mu\text{m/m}$ at 28 days [16].

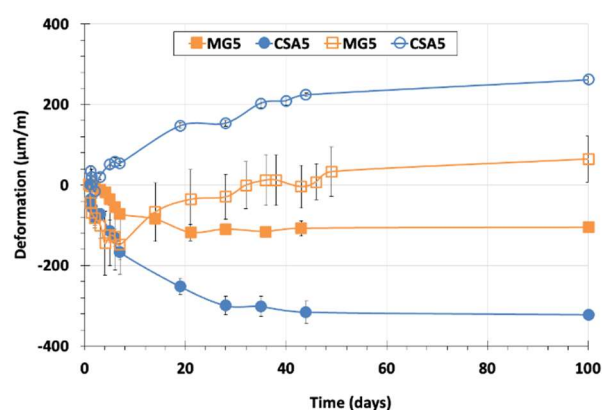


Fig. 4. Autogenous deformation (closed symbols) and total deformation under water curing from 28 days (open symbols).

For the total deformation presented in Figure 4, all mixtures were stored in a humidity-controlled room (95 % R.H.) until 28 days. At two days, the specimens exhibited a mass loss of less than 0.5 %, attributable to hydric exchanges between the specimens and their environment. Subsequently, the specimens gradually began to regain their mass.

The addition of 5% EAs reduces matrix shrinkage. MG5 exhibits slow shrinkage during the first week, reaching a deformation of $-150\text{ }\mu\text{m/m}$ at 7 days. In contrast, CSA5 shows minimal shrinkage at 1 day ($-16\text{ }\mu\text{m/m}$), which is then offset by rapid matrix swelling, resulting in a positive deformation of $+54\text{ }\mu\text{m/m}$ at 7 days. The reference mortar without expansive agents shrinks rapidly during the first 7 days ($-330\text{ }\mu\text{m/m}$) [16]. In a highly humid environment (95 % R.H.), the hydration of CSA is significantly faster compared to the slower hydration of MgO [16]. The formation of ettringite generates swelling pressures within the matrix, leading to a rapid reduction in the total shrinkage of CSA5 at an early age.

After 7 days, MG5 continues to significantly reduce its total shrinkage, reaching $-29\text{ }\mu\text{m/m}$ at 28 days, at a faster rate than CSA5, which exhibits a deformation of $+150\text{ }\mu\text{m/m}$ at 28 days. This phenomenon is related to the continuous formation of brucite due to MgO hydration [16]. By comparison, the reference mortar without expansive agents decreases very slowly and reaches $-280\text{ }\mu\text{m/m}$ at 28 days [16].

Under water curing (WC) conditions (beyond 28 days), the addition of 5% EA slightly enhances the continuous swelling of both MG5 and CSA5. The total deformation remains superior for CSA. For example, its value at 44 days equals $225\text{ }\mu\text{m/m}$ and $5\text{ }\mu\text{m/m}$ for MG5 and CSA5, respectively.

4.2 Healing Capacity

The healing capacity is evaluated through crack width monitoring on the specimen surfaces (2D measurement) and water permeability testing (3D measurement). To determine the healing kinetics, these measurements are performed on cracked specimens at the time of cracking (0D) and after various curing durations: 7 days (7D), 25 days (25D), and 112 days (112D). Additionally, the

main healing products are identified both on the crack surface and within the crack.

The average residual crack width (CW) obtained after the splitting test (at 0D) and measured on the surfaces of the specimens' ranges from 155 to 385 μm . The evolution of CW as a function of their initial values (at 0D) is shown in Figures 5 and 6 for both studied repair mortars. The kinetics of crack healing is primarily influenced by the initial CW. Mixtures with EAs demonstrate complete healing of the majority of cracks within the range of 50-250 μm after 25 days. Beyond this range, mixtures with EAs exhibit faster and more extensive crack healing compared to the reference mortar without expansive agents [16]. Therefore, the addition of EA to cement-based mortars appears to enhance the healing potential of larger cracks.

Given that the crack is not uniform along the height of the specimen [5], it is important to consider crack shape parameters (width, tortuosity, constrictivity) that affect transport properties [17]. This is achieved through the water permeability test.

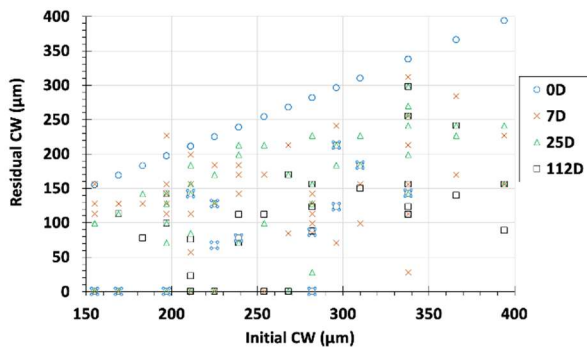


Fig. 5. Crack Width (CW) evolution for MG5.

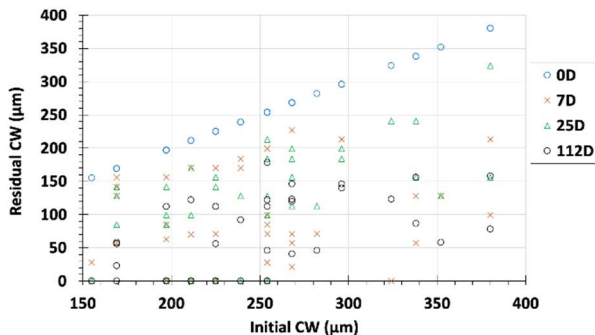


Fig. 6. Crack Width (CW) evolution for CSA5.

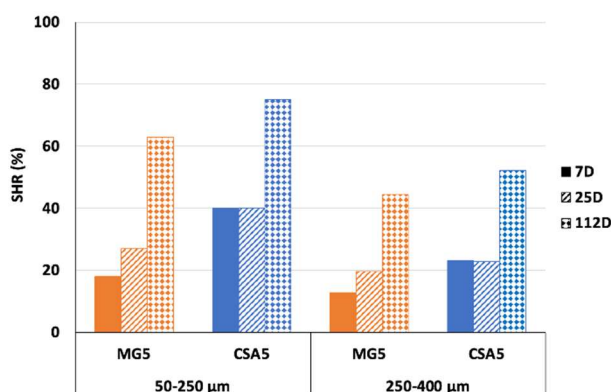


Fig. 7. Self-healing rate evolution for two crack width rates.

Two initial water flow (WF) ranges are selected: [0.001-0.03] l/min and [0.03-0.07] l/min. The corresponding crack width (CW) ranges for these WF ranges are [50-250] μm and [250-400] μm , respectively. The Self-Healing Rate (SHR) as a function of the initial CW is presented in Figure 7:

- For an initial CW of [50-250] μm : After 7 days of water curing, the SHR is 40 % for CSA5 and 18 % for MG5. The healing process continues, and by 112 days, the SHR reaches 75 % for CSA5 and 63 % for MG5. Therefore, the addition of CSA significantly improves the healing process both at early days after cracking and at the long term.
- For an initial CW of [250-400] μm : After 7 days of curing, the SHR is 23 % for CSA5 and 13 % for MG5. After 112 days of water curing, the SHR is equal to 52 % and 44 %, respectively. For larger crack width, mortar with CSA always presents a better healing capacity, but the global performance of the swelling agents is more limited. It is related to its swelling capacity (Figure 4).

During the monitoring of crack width on the specimen surfaces, the formation of white products was observed along the cracks for all the studied mixtures. These products are primarily carbonate-containing phases. Additionally, a small amount of brucite was detected among the white products of mortar with MgO. The morphology of the carbonates on the crack surface was examined using SEM-EDX. These observations confirmed the presence of various types of products, including magnesian calcite and aragonite.

EDX analyses performed inside the cracks identified the internal self-healing products. The results confirmed the presence of C-S-H as a common healing product. Other products detected in lower quantities included ettringite in both studied mortars and M-S-H in mortar with MgO.

The main objective of this section is to evaluate the benefits of EAs to the self-healing process of cracks. It is concluded that self-healing is driven by three mechanisms: carbonation, additional hydration, and matrix expansion. The first two mechanisms are observed in all studied mixtures for crack widths ranging from 50 to 250 μm . The last mechanism is beneficial to limit the largest crack width as shown by CSA5 (Figure 7).

4.3 Concrete Support Roughness

For the chemically treated surfaces (DS), the average distance between irregularities λ is slightly inferior to that of the ground surface (GS) (Table 3). However, the amplitude $2a$ is more than three times greater. This explains why the mean profile depth (MPD) is higher for DS compared to GS. These results also show that MPD is more affected by the depth of the roughness.

Table 3. Roughness characteristics (mm) of the chemically treated surface (DS) and the ground surface (GS)

	GS	DS
MPD	0.33	1.69
λ	4.8	3.9
$2a$	0.5	1.7

4.4 Interface Properties

The results on the bond strength are presented in Figure 8. For both studied mortars, the best bond strength is achieved with the surfaces treated with the setting retarder (DS), which have the greatest roughness depth. It allows a better mechanical interlocking of the mortars with the concrete.

Bond strength also increases with relative humidity, with the best achieved at 85 % R.H. This condition improves the hydration process of the repair mortar at the interface. At 75 % R.H. and for ground surfaces, the resistance of the interface between MG5 and the concrete is very low and does not resist the stresses associated with coring. It can be explained by a less good mechanical interaction between the repair mortar and the sound concrete.

Whatever the preparation conditions, CSA5 mortar demonstrates better bond strength performance compared to MG5 mortar. For example, the bond strength of specimens with the chemically treated surfaces (DS) and an 85 % R.H is equal to 4.4 and 3.3 MPa for CSA5 and MG5, respectively. This value is superior to the value recommended by the European standard EN 1504-3 [10] for the structural application (R4 class).

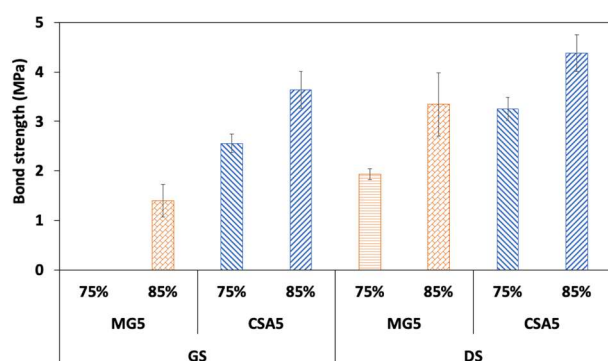


Fig. 8. Bond strength of the studied mortars.

5 Conclusions

This study has evaluated the mechanical performance, self-healing capacity, and interface properties of repair mortars containing expansive agents. The studied mortars meet the requirements of the European standard EN 1504-3, achieving a compressive strength of ≥ 45

MPa and classified as R4, suitable for structural applications.

The addition of 5% expansive agents significantly reduces autogenous shrinkage. Specifically, CSA5 exhibits rapid early-age swelling due to the formation of ettringite, while MG5 shows a slower but continuous reduction in shrinkage over time, attributed to the formation of brucite. Under water curing conditions, both mixtures demonstrate enhanced swelling, with CSA5 performing better overall.

The self-healing capacity of the mortars was assessed through a 3D test: a water permeability testing. Mixtures with expansive agents showed superior healing. Notably, CSA5 exhibited better healing performance due to more significant swelling. The healing process is driven by carbonation, additional hydration, and matrix expansion, with expansive agents enhancing the healing of larger cracks. SEM-EDX analysis confirmed the formation of various healing products, including carbonates, C-S-H, ettringite, and M-S-H.

The study also highlighted the importance of surface preparation on bond strength. A greater roughness and a relative humidity equal to 85% R.H. improve the mechanical interlocking between the sound concrete and the repair mortar and enhance the hydration process at the interface, respectively.

Overall, CSA5 demonstrated better interface performance compared to MG5, with bond strengths exceeding the recommendations of EN 1504-3 for structural applications. These findings underscore the potential of CSA in developing durable and effective repair mortars with enhanced self-healing capabilities.

References

1. D. Breyse, Introduction à la problématique des risques en Génie Civil, [online], Available: <http://www.unit.eu/cours/cyberrisques/rdc/res/Polycopierdc.pdf> (2009)
2. M. Lechani, S. kenai, N. E. Hannachi, Diagnostic des causes de dégradation des ouvrages en béton armé, [online], Available: <http://www.entp.edu.dz/revue/files/article/15/article%207.pdf>
3. F. Benboudjema, A. Darquennes, “Fissuration par retrait gêné dans les ouvrages en béton armé”, *Techniques de l’Ingénieur* (2015).
4. M. Roig-Flores, S. Moscato, P. Serna, L. Ferrara, “Self-healing capability of concrete with crystalline admixtures in different environments”, *Construction and Building Materials*, 6 (2015).
5. K. Olivier, A. Darquennes, F. Benboudjema, R. Gagné, “Early-age self-healing of cementitious materials with ground granulated blast-furnace slag under water curing”, *Journal of Advanced Concrete Technology*, 14 (2016)
6. T. Qureshi, A. Al-Tabbaa, “The effect of magnesia on the self-healing performance of portland cement with increased curing time”, 1st

International Conference on Ageing of Materials & Structures (2014)

7. T. Qureshi, A. Kanellopoulos, A. Al-Tabbaa, “Autogenous self-healing of cement with expansive minerals: Impact in early age crack healing”, *Construction and Building Materials*, 192 (2018)
8. P. Zhang, Y. Dai, W. Wang, J. Yang, L. Mo, W. Guo, J. Bao, “Effects of magnesia expansive agents on the self-healing performance of microcracks in strain-hardening cement-based composites”, *Materials Today Communications*, 25, (2020).
9. M. A. Sherir, K. M. Hossain, M. Lachemi, “The influence of MgO-type expansive agent incorporated in self-healing system of engineered cementitious composites”, *Construction and Building Materials*, 149 (2017)
10. NF EN 1504-3, Produits et systèmes pour la protection et la réparation des structures en béton - Définitions, exigences, maîtrise de la qualité et évaluation de la conformité - Partie 3 : réparation structurale et réparation non structurale (2006)
11. NF EN 206+A2/CN, Béton - Spécification, performance, production et conformité - Complément national à la norme NF EN 206+A2 (2022)
12. EN 196-1, Méthodes d'essais des ciments. Détermination des résistances mécaniques (1990)
13. NF EN 1542, Produits et systèmes pour la protection et la réparation des structures en béton - Méthodes d'essais - Mesurage de l'adhérence par traction directe (1999)
14. NF EN 13036-1, Caractéristiques de surface des routes et aérodromes - Méthodes d'essai - Partie 1: mesurage de la profondeur de macrotexture de la surface d'un revêtement à l'aide d'une technique volumétrique à la tâche (2010)
15. N. J. Bélaïr, Contribution à la mise au point d'une procédure de caractérisation quantitative des surfaces en béton en vue de travaux de réfection, Master Thesis, Laval University, Canada (2005)
16. L. Ammar, Self-healing capacity of cementitious materials: Enhancement with expansive agents and mineral additions, PhD Thesis, INSA Rennes, France (2022)
17. A. Darquennes, K. Olivier, F. Benboudjema, R. Gagné, “Self-healing at early-age, a way to improve the chloride resistance of blast-furnace slag cementitious materials”, *Construction and Building Materials*, 113 (2016)